J. Magn. Soc. Jpn., 30, 624-629 (2006) <Paper>

Monolithically Integrable Semiconductor Active Waveguide Optical Isolators

H. Shimizu*,***, T. Amemiya*,***, M. Tanaka**,***, and Y. Nakano*,***

*Research Center for Advanced Science and Technology, The University of Tokyo, *4-6-1 Komaba, Meguro-ku, Tokyo 153-8904, Japan*

**Department of Electronic Engineering, The University of Tokyo, *7-3-1 Hongo, Bunkyo-ku, Tokyo 113-8656, Japan*

***Japan Science and Technology Agency, SORST

We have proposed, simulated, fabricated and experimentally demonstrated monolithically integrable semiconductor active waveguide optical isolators based on the nonreciprocal loss at an optical telecommunication wavelength range of 1530-1560nm. The semiconductor active waveguide optical isolators are composed of semiconductor optical amplifier (SOA) waveguides and ferromagnetic metals. In transverse electric (TE) mode semiconductor active waveguide optical isolators composed of InGaAsP SOA waveguides and Fe thin films, we demonstrated 14.7dB/mm optical isolation at the wavelength of 1550nm and 10dB/mm isolation over entire wavelength range of 1530-1560nm. In transverse magnetic (TM) mode semiconductor active waveguide optical isolators, we used epitaxially grown MnAs thin films as top ferromagnetic electrodes, and demonstrated stable electrode performance and 8.8dB/mm optical isolation. Based on these demonstrations, we can realize monolithic integration of optical isolators with edge-emitting semiconductor laser diodes and polarization insensitive semiconductor active optical isolators. We also discussed the problems and solutions of our semiconductor active waveguide optical isolators at present stage.

Key words: Fe, InGaAsP, InGaAlAs, nonreciprocal loss, photonic integrated circuit, semiconductor optical amplifiers, waveguide optical isolator, epitaxial ferromagnet, MnAs

1. Introduction

Synthesis of *III-V Semiconductor / Ferromagnetic metal or semiconductor* hybrid structures is one of the hot topics in "semiconductor spintronics". Semiconductor waveguide optical isolators are ones of the most promising applications of III-V semiconductor / ferromagnet hybrid systems, which combine optical nonreciprocal property by ferromagnetic materials and light emission / amplification characteristics by III-V optoelectronics. Optical isolators are indispensable devices to prevent edge-emitting telecommunication semiconductor lasers from unexpected light reflections and assure their stable operations. Commercially available optical isolators are composed of "free space" Faraday rotators and linear polarizers, and are not compatible with semiconductor lasers, because it is difficult to epitaxially grow or deposit high quality magneto-optic materials, such as ferrimagnetic rare earth iron garnets, on III-V optical compound semiconductor substrates, such as InP and GaAs. Semiconductor waveguide optical isolators, which can be monolithically integrated with edge-emitting semiconductor lasers and other III-V optoelectronic devices, are awaited for reducing overall system sizes. Monolithic integration of conventional "free space" optical isolators with InP based edge-emitting semiconductor laser diodes is considered difficult because of the above problems. Despite these challenges, monolithically integrable waveguide optical isolators have been sought for a long time [1]. To realize monolithically integrable optical isolators, we have proposed semiconductor active waveguide optical isolators based on the nonreciprocal loss. The semiconductor active waveguide optical isolators based on the nonreciprocal loss are composed of semiconductor optical amplifier (SOA) waveguides and ferromagnetic metals [2-4]. The nonreciprocal loss is based on the transverse magneto-optic Kerr effect inside the magneto-optic waveguide. The nonreciprocal loss is brought about by the reflection of light at the interface between the ferromagnetic metal and the SOA

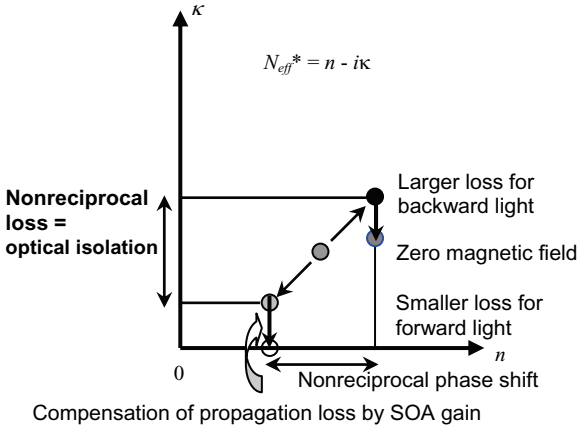

Fig.1 Schematic operation principle of the semiconductor active waveguide optical isolators based on the nonreciprocal loss.

waveguide. There is a difference in the complex reflection coefficient (both the amplitude and phase change) at the laterally magnetized ferromagnetic upper electrode / SOA waveguide interface between the forward and backward propagating light. Please note that this configuration between the magnetization and the light propagation direction is not the Faraday configuration, but the Voigt configuration. In other words, the backward propagating light suffers from stronger absorption loss by the ferromagnetic metal than the forward propagating light. The SOA gain compensates the forward propagation loss. Under these conditions, this SOA waveguide with ferromagnetic metal works as an optical isolator, as schematically shown in Fig. 1. The SOA gain wavelength band determines the operational wavelength range, which is typically 30~40nm for SOAs with InGaAsP multiple quantum well (MQW) active layer. Because the principle of this novel waveguide optical isolator is completely different from that of conventional "free space" optical isolators based on Faraday rotation, *polarizers are not necessary*. This is a great advantage over conventional "free space" optical isolators, and allows monolithic integration with edge emitting semiconductor lasers. Also, the realization of semiconductor waveguide nonreciprocal devices allows us the previously impractical cascading of various semiconductor optoelectronic devices in more powerful highly functional photonic integrated circuits. In this paper, we report design, fabrication and demonstration of both transverse electric (TE) mode and transverse magnetic (TM) mode semiconductor active waveguide optical isolators based on the nonreciprocal loss.

2. TE-mode InGaAsP active waveguide optical isolators

First, we describe design, fabrication, and demonstration of TE-mode semiconductor active waveguide optical isolators. Our TE-mode semiconductor active waveguide optical isolators are composed of InGaAsP SOA waveguides and ferromagnetic metal Fe. An operational wavelength range was designed at optical telecommunication wavelength range of $\lambda \sim 1550$nm. To achieve TE-mode nonreciprocal loss, the magnetization vector of the ferromagnetic metal Fe is aligned parallel to the magnetic field vector $\boldsymbol{H}$ of the TE-mode light, perpendicular to both the waveguide and the substrate (Voigt configuration). Therefore, we deposited Fe thin films on one of the InGaAsP SOA waveguide sidewalls by an electron-beam evaporator with substrates tilted. The SOA layer structure was grown by metal-organic vapor phase epitaxy (MOVPE) and composed of a (100) n^+ doped InP substrate, a 300nm-thick n-InP buffer layer, a 50nm-thick undoped InGaAsP guiding layer, a 14 undoped MQW active layer (10nm-thick InGaAsP compressively strained quantum wells with 10nm-thick InGaAsP tensile strained barriers), a 50nm-thick undoped InGaAsP guiding layer, a 1.5μm thick p-doped InP cladding layer, and a p^+InGaAs contact layer. The deep etched waveguides were fabricated by a Cl_2 / Ar inductly coupled plasma (ICP) reactive ion etching. The waveguide width is 1.5μm. The Fe layer was separated from InGaAsP active layer by 30nm-thick TiO_2 layer to adjust the propagation loss by the Fe layer. Fig. 2 shows the cross-sectional image of the fabricated device by a scanning electron microscope. We have theoretically calculated optical isolation of our TE-mode semiconductor active waveguide optical isolators with the above waveguide layer structure. We calculated the propagation loss by the effective index method and the nonreciprocal loss by the perturbation theory. Here, the nonreciprocal loss $\Delta\alpha$ is expressed through following equations,

$$\Delta\alpha\ [\mathrm{dB/mm}] = 0.02\ \mathrm{Log}[e]\ k_0\ \ \mathrm{Im}[\Delta n_{eff,\,TE}] \qquad (1)$$

$$\Delta n_{eff,TE} = \frac{i}{k_0} \frac{\iint_{Fe} \frac{\varepsilon_{yz}}{\varepsilon} H_x^* \frac{\partial H_x}{\partial y} dxdy}{\iint_{all} |H_x|^2 dxdy} \qquad (2)$$

where k_0 is the wavenumber in vacuum, $\Delta n_{eff,\,TE}$ is the TE like mode effective refractive index change between the forward and the backward propagating light, ε is the dielectric constant, ε_{yz} is the off-diagonal component of the dielectric tensor which is unique to magnetic materials, and H_x is the x-component of the TE like mode magnetic field vector. The refractive indices of the TiO_2 and Fe at 1550nm are assumed to be 2.1 and $3.17 + 5.27i$ respectively. ε_{yz} of Fe at 1550nm is assumed to be $3.15 + 1.8i$ [5, 6]. Fe can provide the largest magneto-optic effect and smallest propagation loss among the elemental transition metals at λ = 1550nm. A nonreciprocal loss (optical isolation) as high as 17.5dB/mm, was predicted for 1550nm TE-like mode light by our simulations. This value corresponds

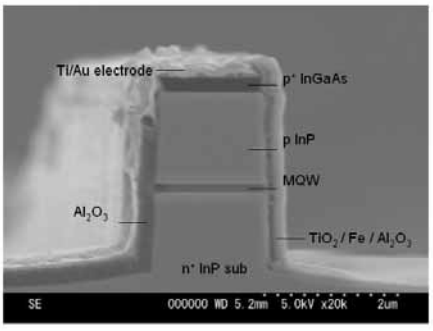

Fig. 2 A cross-sectional scanning electron microscope (SEM) image of the fabricated InGaAsP / InP SOA waveguide with an Fe layer on a waveguide sidewall.

to a device length of 1.71mm for 30dB isolation.

Fig. 3 shows the nonreciprocal propagation characteristics of the fabricated device of 0.7mm-long with cleaved facets under a fixed permanent magnetic field 0.1T. Here, the bias current of the SOA is 100mA. The devices were kept at 10°C. The single mode tunable laser diode light was of wavelength 1530-1560nm, intensity 5dBm, and coupled in and out of the device through lensed optical fibers. The transmitted light was examined with an optical spectrum analyzer to separate out the transmitted light from the amplified spontaneous emission of the SOA. We changed the propagation direction by two mechanical optical switches and optical circulators. The light polarization was adjusted by in-line polarizers. In the TE-mode, the propagation light intensity was altered by a difference of 14.7dB/mm between the forward and the backward traveling light. However, the intensity change was very small (1dB) for TM-mode.

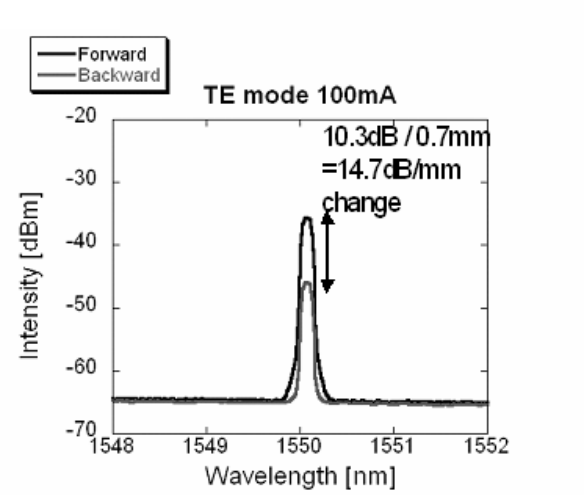

Fig. 3 The measured nonreciprocal loss of the fabricated device for the λ = 1550nm TE-mode at the 100mA bias under a magnetic field of 0.1T.

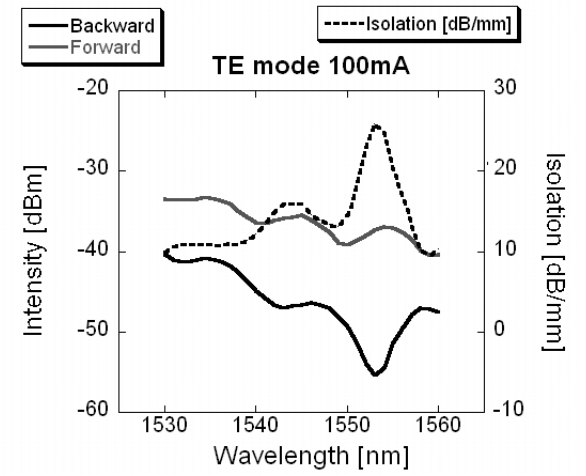

Fig. 4 Wavelength dependence of the optical transmission and the optical isolation ratio at the 100mA bias.

Because this device operates TE-mode, this polarization dependence is a clear evidence of the nonreciprocal loss, which is schematically shown in Fig. 1 [7].

Fig. 4 shows the wavelength dependence of the TE-mode propagation intensity and isolation ratio at a 100mA bias. Greater than 10dB/mm nonreciprocal attenuation was demonstrated over the entire wavelength range of 1530-60nm. Some peaks were observed in the transmitted light intensity and isolation ratio spectra for TE-mode. The isolation ratio was particularly large (25.3dB/mm) at lower bias current I = 100mA and 1553nm. The cause of the isolation ratio fluctuation is not entirely clear, though the uncoated cleaved facets are one likely contribution. The propagation loss increased monotonically with the wavelength from 1530nm to 1560nm. Since the gain peak of the MQW active layer was 1540nm, this monotonic increase of the propagation loss is attributed to the larger optical absorption of the Fe layer at longer wavelengths [8].

At present, the device has large propagation loss (10-15dB) by sidewall roughness of the deep-etched waveguide as shown in Fig. 2. We can reduce the propagation loss by improved reactive ion etching process.

3. TM mode semiconductor active waveguide optical isolators using epitaxially grown MnAs ferromagnetic electrodes

To realize polarization insensitive waveguide optical isolators, it is necessary to realize and combine TE- and TM-mode nonreciprocal propagations. We have also demonstrated TM-mode semiconductor active waveguide optical isolators. To achieve TM-mode nonreciprocal loss, the magnetization vector of the ferromagnetic metal is aligned parallel to the magnetic field vector $\boldsymbol{H}$ of the TM-mode light, which is perpendicular to the light propagation and parallel to the substrate. In other words, the configuration between the magnetization and the light propagation is 90° rotated compared with the TE-mode semiconductor active waveguide optical isolators in the previous section. Ferromagnetic metals are placed on top of SOA waveguides and work as not only magneto-optic materials but also top electrodes in TM-mode semiconductor active waveguide optical isolators. Therefore the ferromagnetic metals must provide large nonreciprocal loss and low-resistive top electrode contact for the p^+InGaAsP contact layer. So far, TM-mode semiconductor active waveguide optical isolators have been demonstrated using polycrystalline elemental ferromagnetic metals Fe, Co, and Ni [9-12]. However, elemental ferromagnetic metals are not always suitable for this purpose. For example, Fe

brings schottkey contacts although the magneto-optic effect of Fe is strongest among transition metals. Upon annealing process to decrease the electrode contact resistance, undesired not-ferromagnetic compounds such as FeAs are produced at the electrode interface, hence reduces the nonreciprocal loss. To solve these problems, we fabricated TM-mode semiconductor active waveguide optical isolators with epitaxially grown MnAs ferromagnetic electrodes. MnAs is a ferromagnetic compound metal with hexagonal NiAs structure and its Curie temperature 40°C. MnAs thin films can be epitaxially grown on (100) GaAs and InP substrates by molecular-beam epitaxy (MBE) [13-15]. Atomically flat and thermodynamically stable interfaces can be obtained between MnAs and GaAs. Therefore, epitaxially grown MnAs thin films are suitable to realize stable ferromagnetic top electrode / p^+InGaAsP contact layer interface with low electrode contact resistance.

The SOA layer stack was grown by MOVPE and composed of a (100) n^+ InP substrate, a 200nm-thick

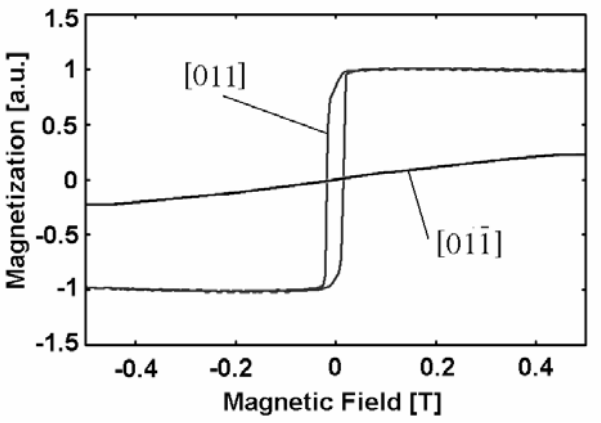

Fig. 5 The magnetization characteristics of the MnAs top electrode of the fabricated TM-mode semiconductor active waveguide optical isolator at room temperature.

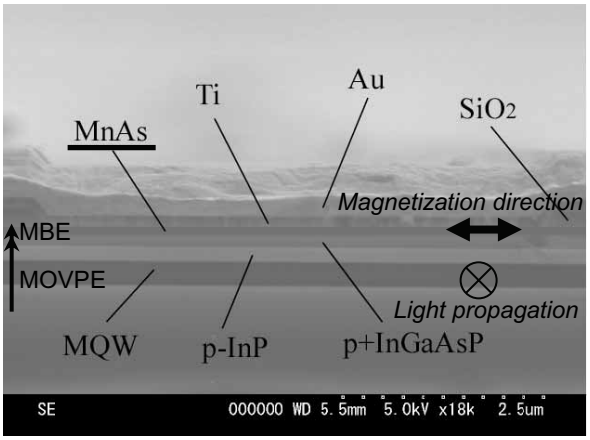

Fig. 6 A cross-sectional SEM image of the fabricated TM-mode semiconductor active waveguide isolator using an epitaxially grown MnAs thin film as a top ferromagnetic electrode.

n-InP buffer layer, a 100nm-thick InGaAlAs lower waveguide layer, a 5 MQW active layer (tensile strained InGaAs quantum wells (-0.4%, 13nm) with six compressively strained InGaAlAs barriers (+0.6%, 8nm) for the TM-mode amplification), a 100nm-thick InGaAlAs upper waveguide layer, a 200nm-thick p-InP cladding layer, and a 200nm-thick p^+ InGaAsP contact layer. The photoluminescence peak wavelength of the MQW was 1540nm. The p-InP upper cladding layer is thinner than that of normal SOAs, to obtain a larger optical confinement factor in the epitaxially grown MnAs thin film ferromagnetic top electrode, and a large nonreciprocal loss. External magnetic field was applied perpendicular to the light propagation direction and parallel to the MnAs thin film. After taking the substrates out of the MOVPE reactor, we introduced them to the MBE chamber for the growth of MnAs thin films. Before growing MnAs thin films, the substrate was heated up to 500-600 °C for thermal cleaning. Then the substrate was cooled to 200 °C and the growth of MnAs thin films was started with the growth rate of 80nm/hour. The MnAs layer thickness is 100nm. Fig. 5 shows the magnetization characteristics of our MnAs thin film at room temperature. The magnetization was measured by alternating gradient force magnetometry (AGFM). When the applied magnetic field was along the [011] of the InP, the MnAs thin film showed almost perfectly square hysteresis characteristics. The coercive field is as low as 0.017T, which can be easily applied by permanent magnets. However, when the applied magnetic field was along the [01-1] of InP, no hysteresis loop was observed and the magnetization did not saturate even at 0.5T. This strong uniaxial magnetic anisotropy of the MnAs electrode is consistent with MnAs thin films grown on (100) GaAs or InP substrates [14, 15]. We thus fabricated the waveguide stripes parallel to the [01-1] of the InP substrate, and the magnetic field was applied parallel to the [011] of the InP substrate. We fabricated 5.5μm width stripe window openings by photolithography for gain guiding waveguide. Then, Ti / Au thin films were deposited by an electron-beam evaporator for upper electrode. Fig. 6 shows the cross sectional image of the fabricated device by scanning electron microscopy.

We measured the propagation characteristics of the fabricated device under a 0.1T permanent magnetic field at 15°C. The device was cleaved to 0.6mm long and facets were left uncoated. The bias current was 100mA. An external magnetic field was applied by a permanent magnet along the [011] of the InP substrate. The laser diode light was of wavelength 1540nm, intensity 5dBm. The required voltage for 100mA bias current was 1.5V, which is much lower than that of semiconductor active waveguide optical isolators with polycrystalline Ni / Fe ferromagnetic electrodes [10]. Fig. 7 shows the propagation characteristics for the TM-mode at 1540nm. In the TM-mode, the output light intensity changed by a difference of 5dB / 0.6mm =

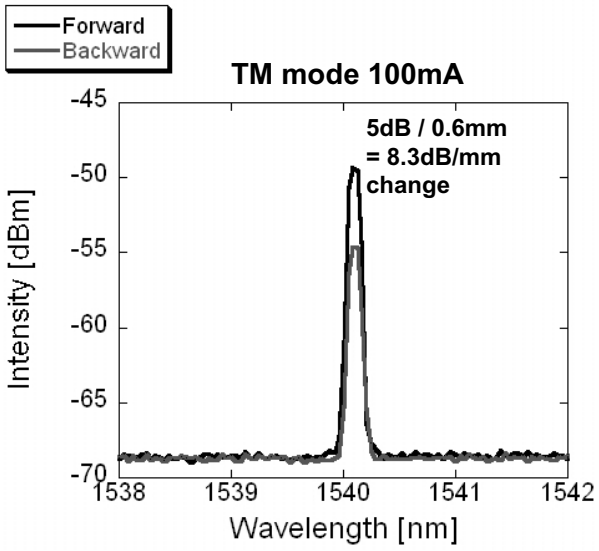

Fig. 7 TM-mode nonreciprocal propagation characteristics of the fabricated device of Fig. 6 at λ = 1540nm.

8.3dB/mm between the forward and backward traveling light.

At this stage, the forward propagation loss is large (approximately 50dB), as shown in Fig. 7. The origins of the forward propagation loss are 1) the absorption loss from the MnAs electrode (approximately 25dB), 2) the coupling loss between the lensed optical fiber and the waveguide (10dB/facet), 3) weak lateral optical confinement due to the gain guiding structure, and 4) insufficient SOA gain to fully compensate the absorption loss from the MnAs electrode. By using larger SOA gain materials and index guiding waveguide structure, it is possible to reduce the forward propagation loss.

It is true that the Curie temperature of MnAs (40°C) is slightly higher than room temperature, which can cause the temperature unstability of the semiconductor active waveguide optical isolators upon the current injection of 100mA. However, when the semiconductor active waveguide optical isolator is monolithically integrated with temperature controlled semiconductor laser diodes (typically 20°C), the temperature unstability problem can be partially solved. Furthermore, by using MnSb thin film ferromagnetic top electrode instead of MnAs, temperature characteristics of magneto-optic properties can be improved. Curie temperature of MnSb is 625K, which is much higher than room temperature, and magneto-optic effect of MnSb is stronger than MnAs owing to stronger spin-orbit interaction. MnSb has the same crystal structure as that of MnAs, and epitaxial growth of MnSb thin films on (100) GaAs substrates and their magneto-optic properties have been reported [17-19]. The use of MnSb ferromagnetic electrode can improve the waveguide optical isolator characteristics.

4. Summary

We have designed, fabricated and successfully demonstrated TE- and TM- mode monolithically integrable semiconductor active waveguide optical isolators based on the nonreciprocal loss. In TE mode semiconductor active waveguide optical isolators composed of InGaAsP SOA waveguides and Fe thin films, nonreciprocal loss of 14.7dB/mm was demonstrated at λ=1550nm. By further improvement of the waveguide optical isolator performance (larger nonreciprocal loss and smaller insertion loss), waveguide optical isolator monolithically integrated semiconductor laser diodes can be demonstrated. Furthermore, we demonstrated TM-mode semiconductor active waveguide optical isolators composed of InGaAlAs SOA waveguides and MnAs epitaxially grown ferromagnetic electrodes and 8.3dB/mm nonreciprocal propagation was demonstrated at λ=1540nm By using molecular-beam epitaxy (MBE) grown MnAs electrode, we successfully realized thermodynamically stable ferromagnetic metal electrode / p^+InGaAsP interfaces with low contact resistances, and the optical isolation ratio and the insertion loss were improved compared with the devices with Ni/Fe polycrystalline electrodes. Although the nonreciprocal loss (optical isolation) of our TE and TM mode semiconductor waveguide optical isolators (~10dB) is lower than conventional free space optical isolators (40~50dB), and the insertion loss of our devices are larger than conventional free space optical isolators at this stage, there are several solutions toward the improvement of these characteristics. Furthermore, by depositing two ferromagnetic layers on a single SOA waveguide (upper and a side), we can realize polarization insensitive semiconductor active waveguide optical isolators.

Acknowledgements This work was partially supported by Industrial Technology Research Grant Program in 2005 from New Energy and Industrial Technology Development Organization (NEDO) of Japan.

References

1) H. Yokoi, T. Mizumoto, N. Shinjo, N. Futakuchi, and Y. Nakano, *Appl. Opt.* **39**, 6158 (2000).
2) M. Takenaka and Y. Nakano, *Proc. 11th Int. Conf. Indium Phosphide and related materials* (1999) 289.
3) W. Zaets, and K. Ando, *IEEE., Photon. Tech. Lett.* **11**, 1012, (1999).
4) H. Shimizu and M. Tanaka, *Appl. Phys. Lett.* **81**, 5248 (2002).
5) P. B. Johnson and R.W. Christy, *Phys. Rev. B.***9**, 5056, (1974).
6) G. S. Krinchik and V. A. Artemjev, *J. Appl. Phys.* **39**, 1276 (1968).
7) H. Shimizu and Y. Nakano, *Jpn. J. Appl. Phys.* **43**, L1561

(2004).
8) H. Shimizu and Y. Nakano, *IEEE. J. Lightwave Tech.* **24**, 38, (2006).
9) M. Vanwolleghem, W. Van Parys, D. Van Thourhout, R. Baets, F. Lelarge, O. Gauthier-Lafaye, B. Thedrez, R. Wirix-Speetjens, L. Lagae, *Appl. Phys. Lett.*, **85**, 3980, (2004).
10) T. Amemiya, H. Shimizu, and Y. Nakano, *Proc of 17th Int. Conf. Indium Phosphide and related materials*, TP-41 (2005).
11) V. Zayets and K. Ando, *Appl. Phys. Lett.*, **86**, 261105, (2005).
12) W. Van. Parys, B. Moeyersoon, D. Van. Thourhout, R. Baets, M. Vanwolleghem, B. Dagens, J. Decobert, O. L. Gouezigou, D. Make, R. Vanheertum, and L. Lagae, *Appl. Phys. Lett.*, **88**, 071115, (2006).
13) M. Tanaka, J.P. Harbison, T. Sands, T.L. Cheeks, G.M. Rothberg, *J. Vac. Sci. & Technol. B***12**, 1091 (1994).
14) M. Tanaka, J.P. Harbison and G.M. Rothberg, *Appl. Phys. Lett.* **65**, 1964 (1994).
15) M. Yokoyama, S. Ohya and M. Tanaka, *Appl. Phys. Lett.* **88**, 012504 (2006).
16) T. Amemiya, H. Shimizu, Y. Nakano, F. N. Hai, M. Yokoyama, and M. Tanaka, *Appl. Lett. Lett.* **89**, 021104, (2006).
17) H. Akinaga, K. Tanaka, K. Ando, and T. Katayama, *J. Cryst. Growth*. **150**, 1144, (1995).
18) S. Miyanishi, H. Akinaga, K. Tanaka, *Appl. Phys. Lett.* **68**, 2890, (1998).
19) K. Sato, H. Ikekame, M. Akita, and Y. Morishita, *J. Magn. Magn. Mater*. **177-181**, 1379, (1998).

Received Jun. 2, 2006; Revised Jul. 18, 2006;
Accepted Aug. 21, 2006